# What's Going On?
## RFI Situational Awareness in GNSS Receivers

PHILLIP W. WARD
NAVWARD GPS CONSULTING

How familiar is this? You switch on your GNSS receiver. It lights up but won't acquire satellites and begin tracking signals. Is the problem in the receiver, the signals, or perhaps the operating environment? This article describes a simple but effective receiver-based method for detecting radio frequency interference (RFI) or jamming that can help answer this question. The design does not require the receiver to be tracking for it to reliably provide RFI situational awareness. Instead, the solution uses measurements obtained from the automatic gain control to help determine the jamming-to-noise power ratio, which serves as the key metric for assessing the RF environment.

I n-band radio frequency interference (RFI) is a serious threat to the reliable operation of GNSS receivers. When the RFI power level is high enough to render the GNSS receiver inoperable, usually no visible external signs appear indicating that anything is out of order; so, the user initially assumes the receiver has experienced an internal failure.

For the purposes of this article, the determination of the presence and seriousness of an RFI problem is called RFI situational awareness. Without the sophistication of built-in *RFI situational awareness* in the GNSS receiver design, the determination of the presence and serious-ness of in-band RFI problems is an extremely inefficient and frustrating process.

Given the growing proliferation of a very large variety of transmitters around the world, the noise floor for GNSS receivers will undoubtedly continue to increase along with the threat of disabling, in-band RFI.

This article describes the design techniques and advantages of built-in RFI situational awareness using a very simple and inexpensive design called a *jamming-to-noise power ratio* (J/N) meter.

One caveat, however: the J/N meter design is "simple and inexpensive" only if this capability is carefully pre-

34    InsideGNSS          SEPTEMBER/OCTOBER 2007          www.insidegnss.com

planned in the design of the original GNSS receiver front-end components, layout, and implementation. Another caveat is that commercial GNSS receiver front-end designs using one-bit analog-to-digital converters (requiring no automatic gain control) do not fit the design prerequisites for this concept.

A retrofit to an existing design is usually impractical. The initial justification for including RFI situational awareness in the design might be based on the significant performance advantages described in this article, but every GNSS receiver user that anticipates or has ever experienced an operational failure due to in-band RFI will greatly value this feature. Certainly, all safety-of-life

GNSS applications and military operations should require it.

## GNSS RF Front-End Architecture

The J/N meter design presented here is implemented in the last stage of a GNSS receiver RF front end architecture — i.e., prior to signal detection.

As is well known, prior to signal detection, the GNSS spread spectrum signal power (S) from each satellite in view is well below the thermal noise power (N). This assumes that the signal has arrived at the receiver antenna input of a receiver located on or near the surface of the Earth and that the antenna gain is in the region of 0 dB, that is, near unity. For a typical example, if S is 30 dB below N, then S/N = S - N = -30 dB at the antenna input.

A key point to remember is that all GNSS spread spectrum signals are designed so that they can be readily acquired and tracked even though the incoming S/N is substantially negative. When in-band RFI jamming power (J) is present, the effective noise level is increased so that the receiver may be unable to acquire and track the GNSS signals in view.

Because the undetected signal is always below the noise level (whether or not J is present), it is impossible to obtain a measure of the composite signal-to-noise power ratio, usually called the *signal-to-noise plus interference power ratio* (SNIR) at the output of the RF front end. This can only be measured by the receiver baseband process after the signal has been acquired (despread) where the SNIR can be positive at baseband if the RFI is not too severe. In other words, it is impossible to measure the SNIR if the RFI power level prevents signal detection at baseband.

The RFI power level might not prevent signal detection if it could be measured before signal acquisition is attempted and the search process is adapted to it. In any case, the good news is that RFI situational awareness is practical and its presence can be accurately measured at the RF front-end output. It cannot be measured with respect to S

but it can be measured with respect to N as J/N.

The jamming-to-noise power ratio is an excellent measure because N is always an acceptable amount of noise for GNSS signal acquisition, with one possible exception. Continuous wave (CW) noise power just below the thermal noise level can be troublesome to the acquisition of the GPS L1 C/A code signals.

## Role of the AGC Amplifier

The J/N measurement takes place in the AGC amplifier, typically the last analog stage in the GNSS receiver RF front end. **Figure 1** is a functional block diagram of a typical digital GNSS receiver RF front end that uses an analog AGC amplifier.

The analog components begin with a right-hand circularly polarized L-band antenna with nearly hemispherical gain coverage. This is followed by an L-band preamp and downconverter and ends with an AGC amplifier at the intermediate frequency (IF). At this point the L-band signal has been amplified by nearly 100 dB and signal-conditioned (filtered).

The gain-controlled analog IF signal is then converted to a digital signal by a sampling and quantization circuit called an analog-to-digital converter (ADC). The digital gain control uses the ADC digital output to close the AGC loop. A digital-to-analog converter (DAC) is required in this feedback loop because the AGC is an analog design, that is, it requires an analog (voltage) gain control.

Each L-band GNSS signal requires separate down-conversion ending in a separate ADC with a digital IF output. Note that at this point only amplification, signal conditioning, and center frequency down-conversion have taken place; so, all of the GNSS signals in view are still buried in noise and, therefore, undetected. The composite signals plus noise spectrum have been band-limited by the signal conditioning process, the center frequency has been lowered to IF, the band-limited signals plus noise have been amplified by nearly 100 dB, and converted to digital IF signals plus noise.

This block diagram does not show that the same digital IF signals are provided to multiple digital receiver channels that are under the control of a receiver processor. If multiple L-band down-conversions to the same IF have been performed — for example the GPS L1 and L2 signals, then each digital receiver selects the appropriate IF to search and track. Also, not shown are the reference oscillator and frequency synthesizer that are required analog components to support the down-con-



FIGURE 1  GNSS Receiver Front End – Analog AGC Amplifier

| Supply Voltage (V) | +5.5V |
|---|---|
| Gain Low End (dB) | −2.5dB |
| Gain High End (dB) | +42.5dB |
| −3 dB BW (MHz) | 500MHz |
| Spectral Noise (nV/rtHz) | 1.84nV/rtHz |
| Gain Accuracy (dB) | ±0.2dB |
| Supply Current | 26mA |
| Package | 14-Lead TSSOP |
| TABLE 1. Analog AGC specification | |

version process and the synchronization of the digital signal processing functions to the real-time analog signals.

The AGC in Figure 1 has its gain controlled by an analog signal. An example of this type of AGC can be seen in **Figure 2**, which illustrates a modern analog AGC circuit design in a functional block diagram. The analog AGC consists of an analog controlled digital attenuator and a fixed gain amplifier. Note that the digital attenuator used to control the amplifier gain in this analog AGC design requires an internal ADC.

The analog AGC amplifier also contains a built-in analog square law detector (rectifier) that can be used to close the AGC feedback loop, but this feature is not used for this application. **Table 1** summarizes the key specifications of the unit. Even with digital attenuators, analog AGC designs usually do not have the dynamic range of a digital AGC design, described next.

## Digital AGC

**Figure 3** is functionally the same block diagram as Figure 1 except that it incorporates a digital AGC, thereby eliminating the DAC in the AGC feedback loop
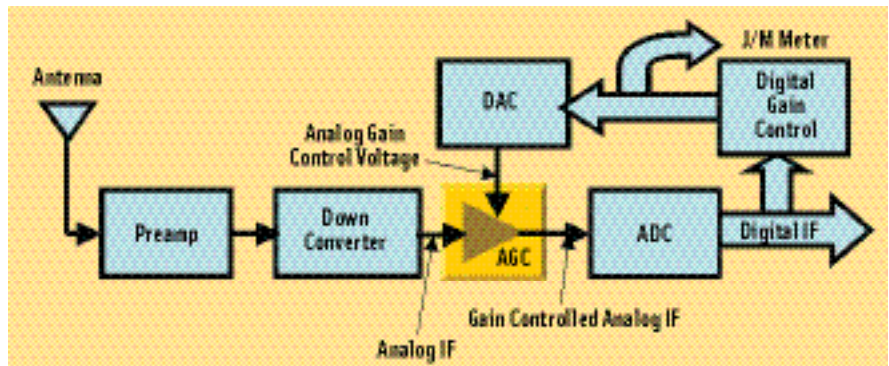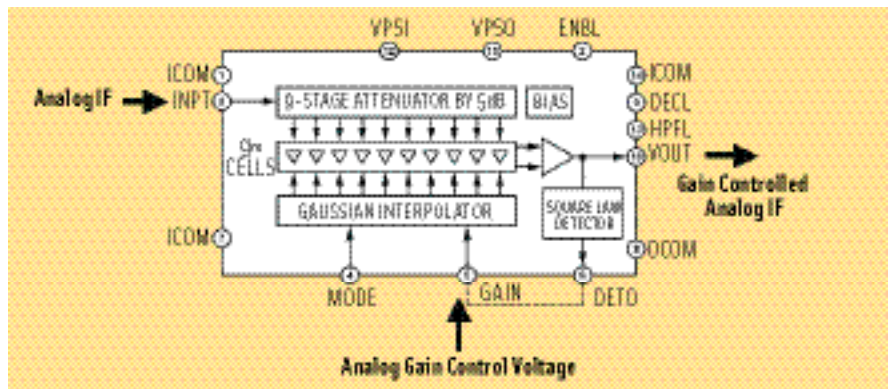


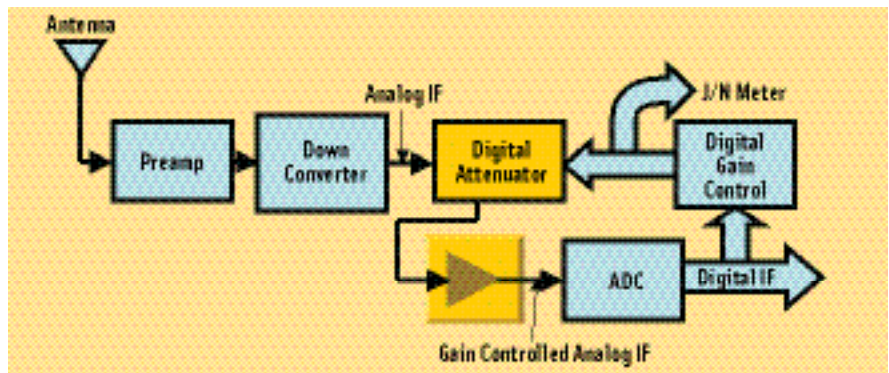FIGURE 2  Functional Block Diagram – Modern Analog AGC Amplifier



FIGURE 3  GNSS Receiver Front End – Digital AGC Amplifier

and the ADC that controls the digital attenuator inside the AGC amplifier. **Figure 4** is representative of a modern digital AGC circuit design shown as a functional block diagram.

The digital AGC consists of a digitally controlled attenuator and fixed gain amplifiers with a provision for the digital control to be transferred to it serially and latched. In an integrated architecture, a parallel-bus transfer would replace the serial digital transfer.

One advantage of the all-digital feedback loop is that the AGC gain can be updated synchronously so that a sub-

stantial part of the gain change occurs between ADC sampling epochs. In this manner, any AGC updates are made in such a fashion that the analog transient has been reduced before analog sampling and digital quantization take place. This is an important feedback stabilizing feature because the AGC attack and recovery times should be as fast as the feedback stability permits for a GNSS receiver designed to operate effectively in the presence of RFI.

**Table 2** summarizes the specifications of the digital AGC. Note that the digital AGC has nearly 60 dB of dynamic
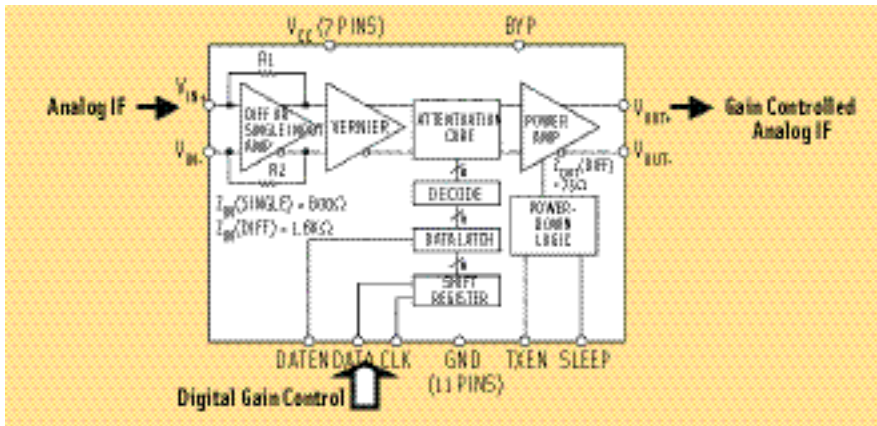
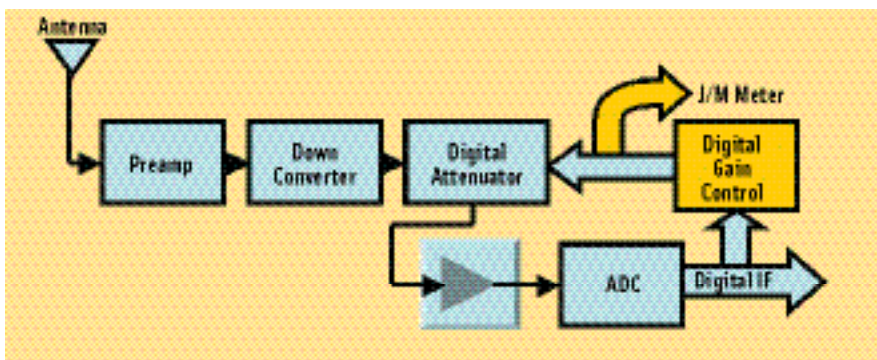FIGURE 4 **Functional Block Diagram – Modern Digital AGC Amplifier**



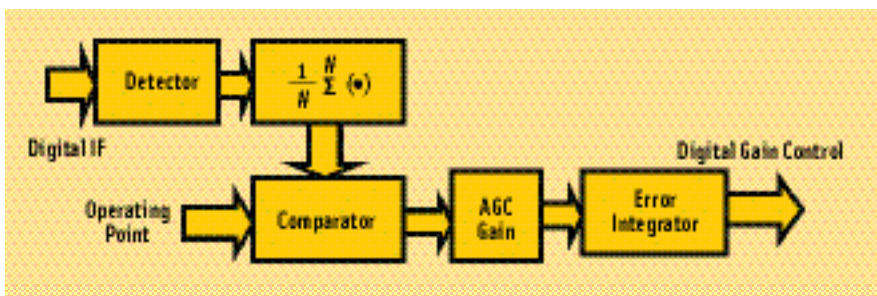FIGURE 5 **GNSS Receiver Front End – Digital Gain Control with J/N Meter**



FIGURE 6 **Functional Block Diagram – Digital Gain Control**

| Supply Voltage (V) | +5V |
|---|---|
| Gain Low End (dB) | –29.5dB |
| Gain High End (dB) | +30dB |
| –3 dB BW (MHz) | 100MHz |
| Spectral Noise (nV/rtHz) | 56nV/rtHz |
| Gain Accuracy (dB) | ±1dB |
| Supply Current | 133mA |
| Package | 28-Lead TSSOP |
| TABLE 2. **Digital AGC specification** | |

range while the analog AGC has 45 dB. Additional AGC dynamic range can be achieved by using switched step attenuators in the gain stages of the down-converter.

The parts of Figures 1 and 3 that are the primary subjects of this paper are the AGC and the digital gain control circuit for the AGC. *These figures also illustrate that the digital gain control for the AGC is the basis for the built-in jamming-to-thermal noise power ratio (J/N) meter.* As will be seen, the J/N meter is a relatively simple by-product of the AGC feedback loop, if, as previously mentioned,

this feature is anticipated as part of the original GNSS receiver design.

**Figure 5** highlights the location of the digital gain control. It illustrates that a by-product of its output is the J/N meter. **Figure 6** shows the functional components of the digital gain control. It consists of a detector (rectifier) followed by a short-term averaging function that provides filtering and sets the attack and recovery rates of the AGC.

The operating point in the comparator sets the rms amplitude level of the AGC so that there is the least quantization noise in the ADC. The optimal

rms amplitude depends on the number of quantization bits used in the ADC design. The AGC gain stage adjusts the signal to match the AGC gain control input. The error integrator provides both memory and smoothing of the digital gain control output.

## J/N Meter: Basic Principles
The basic principle of operation for the J/N meter shown in Figures 1, 3, and 5 relies on the facts that: (1) the GNSS signals are buried in thermal noise prior to the correlation process (detection), and (2) in the absence of RFI, the AGC operating point is set by the thermal noise level, which becomes the reference power level, N.

If the AGC digital gain control changes from N, that change is an indication that the noise level has increased. *This noise increase can only be caused by in-band RFI.* **This RFI level, when it rises above N, can be measured precisely with respect to N by the change in the AGC digital gain control level.** Because the reference level is N then the measurement power ratio is J/N.

As depicted in Figures 1, 3 and 5, the AGC gain is attenuated in the presence of increased RFI. The AGC gain is linear in dB; so, the AGC digital gain control must be multiplied by a predetermined scale factor to convert its level into decibel units. The calibration techniques and the algorithms used in this measurement are described in the following section.

## J/N Meter Calibration & Algorithms
Calibration of the J/N meter requires only two test functions: (1) muting the GNSS receiver RF front end so that no

external RFI can enter from the antenna while the AGC characterizations are performed, and (2) a switch controlled in-band signal that is injected into the RF front end.

Two different signal powers are switched, one low and one high, such that both are above the thermal noise level but within the dynamic range of the AGC. The precise difference in these two signal powers, K, must be determined *a priori*.

Typically, the output signal of an in-band sine-wave signal generator is injected into the muted GNSS RF front end with a precise two-step attenuator. For this technique, the *a priori* constant K is defined as the difference between the two attenuator values in decibels.

These two calibration provisions are simple and can be built in, but they can also be performed at the factory. The disadvantage of the factory calibration is that the accuracy might deteriorate with age or other conditions.

If these two features are built in, the following AGC characterization algorithms are performed as part of the built-in test procedures of the GNSS receiver prior to initial GNSS signal search and acquisition. (The test calibration occurs each time the receiver is powered up along with all other pre-operation test functions. The time taken for this specific test is much less than a second and is imperceptible to the operator.) Otherwise, they are performed at the factory.

The algorithms assume that the AGC is designed so that increasing values of the digital gain control correspond to increasing attenuation; in other words, stronger IF signal power results in larger values out of the digital gain control.

The following characterization steps also assume that control-switched step attenuators are located in the gain stages of the down-conversion portion of the RF front end that provide increased dynamic range for the AGC. If this feature is not present, then assume that the step attenuators are set to zero dB (unity gain).

**AGC Characterization Step 1.** Because the AGC gain (G) is linear in decibels with linear change in digital gain control value (V), then a scale factor (D) relates the two, so that $G = DV$ (dB).

To calibrate D, first isolate the RF front end from the antenna (mute the RF front end), then inject the first (low) signal, and finally read and store the corresponding digital gain control value (V1). Inject the second (high) signal, then read and store the corresponding digital gain control value (V2). Calibrate D as follows:

$$(1)\quad D = K/(V2 - V1)$$

where, *a priori* constant K was defined earlier. Perform this calibration and then store the result for each AGC (each GNSS carrier) tracked by the receiver. It is prudent to use averaged values of V1 and V2.

**AGC Characterization Step 2.** With the RF front end muted, compute the RF front end gain level that corresponds to the thermal noise level at IF ($G_M$) by reading the content of the AGC digital gain control level ($V_M$), then converting the gain value to decibels using D, calculated in Step 1:

$$(2) \quad G_M = DV_M \text{ (dB)}$$

Again, using averaged values of $V_M$ is prudent. Perform this measurement and computation, and then store the result for every step attenuation–level combination (M) that precedes the AGC amplifier.

**AGC Characterization Step 3.** Compute and store every thermal noise level ($N_M$) in decibels, accounting for every step attenuator value ahead of the AGC, by adding the current step attenuation level, $A_M$, to $G_M$ (for example, $A_1 = 0$ dB, $A_2 = 18$ dB, $A_3 = 36$ dB):

$$(3) \quad N_M = G_M + A_M \quad \text{(dB)}$$

This concludes the AGC characterization.

The astute reader will observe that the muting of the GNSS antenna signals to prevent any RFI from corrupting the calibration process removes the effects of the antenna noise contribution to the unjammed noise level of the receiver, thereby decreasing the measured reference noise level. However, this is typically a small order effect of around 1 dB. It can either be neglected or, if the antenna noise temperature is known, the noise contribution can be computed and the effect added to $N_M$.

A more serious effect can occur if the muting point is at the GNSS preamp output. When the antenna/preamp assembly is remotely located, injecting the built-in test signals into the preamp input is not practical.

However, the preamp output can be muted by simply switching off the DC power, which is usually provided by the GNSS receiver via the preamp co-axial cable center conductor. Controlling this feature must be anticipated in the GNSS receiver RF front end design. The ther-

mal noise effect on the characterization cannot be neglected because the preamp effectively determines the receiver noise figure. When the AGC characterization steps are complete, the GNSS receiver is ready for normal operation.

## Measuring J/N Power Levels

This section will now describe the J/N measurement steps during normal operation. *Note that during the normal operation of the GNSS receiver, the in-band RFI level can be measured anytime, including the time prior to initial signal acquisition, even if the GNSS receiver is incapable of signal acquisition because of excessive RFI.*

**J/N Measurement Step 1.** Compute the current RF front end gain level (G) by reading the current content of the AGC digital gain control level (V) and converting the gain value to decibels using scale factor constant, D.

$$(4) \quad G = DV \quad \text{(dB)}$$

It is prudent to use averaged values of V.

**J/N Measurement Step 2.** Assuming that the GNSS signal power is so far below the noise level as to be neglected, compute the current in-band noise level (J), accounting for the current step attenuator setting:

$$(5) \quad J = G + A_M \text{ (dB)}$$

**J/N Measurement Step 3.** Compute J/N using the noise measurement corresponding to the current step attenuator setting determined in Step 2:

$$(6) \quad J/N = J - N_M \quad \text{(dB)}$$

Note that J/N is zero dB when only thermal noise is present and rises by 1 dB for every 1 dB increase in the meter reading above $N_M$.

## Advantages of J/N Meter

The benefits of a J/N meter are all based on the major advantage that this feature provides RFI situational awareness at all times the GNSS receiver is turned on, even if the RFI level is so high that the receiver is incapable of signal acquisition and tracking.

Because the J/N meter is operational prior to initial signal acquisition, it can be used to adapt the search strategy using measured RFI when the jamming level rises above the thermal noise level. The scheme involves adjusting the search dwell time (T) based on the J/N level so that the signal-to-noise power ratio $(C/N)_{dB}$ at the input of the search detector is at or above the level that assures a desired probability of signal detection.

In the following case example, the received signal power levels from all satellites are assumed to be the minimum



©iStockphoto.com/Sean Locke

specified signal power. Assume that a 90 percent probability of detection is desired and a Tong search detector is used. (Chapter 5 of *Understanding GPS: Principles and Applications*, E. Kaplan and C. Hegarty, editors, discusses use of the Tong search detector in this application. See the Additional Resources section at the end of this article for the full citation.)

From this cited reference, setting the Tong detector parameters A = 8, B = 1, and the false alarm probability at $1\times10^{-6}$, then the input $(C/N)_{dB}$ must be about 7 dB to achieve a 90 percent probability of detection ($P_D$). If $(C/N)_{dB}$ = 7 dB and T = 1 ms this corresponds to a baseband carrier-to-noise power ratio in a 1-Hz bandwidth, $(C/N_0)_{dB}$ = 37 dB-Hz. This is because $(C/N_0)_{dB} = (C/N)_{dB} - 10 \log T$, where T is in seconds.

The high quality L1 C/A-code receiver design described in Chapter 5 of *Understanding GPS: Principles and Applica-tions* will be used in this example. This design assumes the minimum specified signal of –158.5 dBW, and an antenna gain toward the satellite of 1.5 dB. This results in a minimum unjammed $(C/N_0)_{dB}$ of about 42 dB-Hz and the relationship J/S = J/N +30.1 dB at IF, assuming that the bandwidth at the IF stage is 18 MHz.

For a C/A code receiver, increasing T beyond 10 ms during initial search produces diminishing returns because of the presence of 50 Hz (20 ms period) data modulation on the carrier signal and the inability to control the phase of the search dwell time with respect to the incoming signal data transition boundaries. Therefore, the adaptive search scheme uses a basic dwell time of 1 ms and intermediate values of 1 ms increments until the upper limit of the search dwell time adaptability is T = 10 ms. For T = 10 ms, inputting the requisite $(C/N)_{dB}$ = 7 dB into the search detector yields a corresponding $(C/N_0)_{dB}$ = 27 dB-Hz.

The J/N meter is used to determine when T is incremented as follows, beginning with T = 1 ms and ending with T = 10 ms. For T = 1 ms, using the computations provided in Chapter 6 of *Understanding GPS: Principles and Applications*, the J/S required to reduce the unjammed $(C/N_0)_{dB}$ from 42 dB-Hz to 37 dB-Hz in this C/A-code receiver design is 29.4 dB, assuming that the RFI is band-limited white noise (BLWN). For T = 10 ms, the J/S required to reduce the unjammed $(C/N_0)_{dB}$ from 42 dB-Hz to 27 dB-Hz is 40.9 dB for BLWN.

Given these assumptions, setting T = 1 ms ensures that $(C/N)_{dB}$ = 7 dB or more is provided to the input of the search detector at baseband until J/S = J/N + 30.1 dB = 29.4 dB at the IF stage. This corresponds to J/N = –0.7 dB. The J/N meter cannot measure RFI power below the thermal noise level, but T does

not have to change until J/N increases to a positive value.

For non-zero J/N measurements, T must be doubled for every 3 dB change in J/N to maintain the same $P_D$. This corresponds to an upper end J/S = J/N + 30.1 = 40.9 dB or J/N = 10.8 dB, which limits this scheme for the L1 C/A-code receiver to a J/N reading of about 11 dB to hold $P_D$ = 90%. As a result of a relatively simple adaptive search strategy based on J/N meter readings, the initial search and acquisition J/S tolerance is about 41 dB — an amazing initial signal acquisition performance for a C/A-code receiver.

Obviously, the J/N meter provides a significant advantage to the GNSS receiver search process. The search scheme significantly outperforms any other design approach and the cost can be low. If there is no J/N meter, then the GNSS receiver search engine design might assume the worst case situation for every initial search condition. This would greatly increase the search time since the vast majority of initial searches are benign. For example, the initial search time of the design just presented would increase by a factor of 10 if it had to assume the worst case RFI level for every initial search.

## Conclusion

The usual assumption for a commercial GNSS receiver is that RFI is not present. The norm is to simply accept the performance limitations of a fixed dwell time code search. But if there were an attempt to improve the search capability without a J/N meter, this would result in an extremely time consuming search if RFI were actually present. This is because T must be increased incrementally each time the search fails since the actual received RFI power is unknown and the cause of the search failure is unknown.

The J/N meter cannot measure signal obscuration or attenuation by buildings or foliage, etc., but these operating conditions are normally observable by the astute GNSS user. If there is signal obscuration or attenuation, the receiver can reasonably deduce that the cause is signal obscuration or attenuation if the search fails but no serious J/N problem is indicated.

Also, the technique described does not locate the source of the RFI or measure the radiated power at the source, but it does measure exactly how much of the received RFI power actually penetrates into the GNSS receiver IF stage. Thus, two different GNSS receivers at the same location, each with an accurate J/N meter, might measure a different level of RFI if the RFI is not exactly in the passband of the receivers. The receiver with the superior RF front end filters will have the least amount of RFI at IF.

A central station could compute an estimate of the RFI source location and its radiated power level of an in-band RFI source using the J/N meter readings of a community of GNSS users. These users would have to be distributed around the RFI source. The diversity of positions and J/N measurements would enable the central station to compute a power gradient map that peaks at the offending location. An example of such a community includes mobile phone users with communications-aided GNSS position location to meet the E911 requirement. Also, any other community dealing with emergency applications such as police officers, FBI agents, Homeland Security agents, and the military.

Once the GNSS receiver is tracking satellites, the J/S level can be estimated from the $C/N_0$ meter reading for each satellite being tracked, but the tracking prerequisite prevents RFI situational awareness of all J/S levels that prevent tracking. Therefore, this method is not reliable in the presence of RFI.

Perhaps the most important advantage of the J/N meter is that the GNSS receiver user can be made aware of the RFI situation under all RFI circumstances. It is a simple extension of the J/N meter design feature to provide the user or the interface system with a "Green/Yellow/Red" meter corresponding to the RF front end signal conditions measured at the receiver IF as being "Operational/Marginal/Disabling," respectively.

## Manufacturers

The analog AGC circuit design shown in Figure 2 and characterized in Table 1 is the AD8367 from **Analog Devices, Inc.**, Norwood, Massachusetts USA. The digital AGC amplifier illustrated in Figure 4 and specified in Table 2 is Analog Devices' AD8325.

## Additional Resources

[1] Kaplan, E., and C. Hegarty, editors, *Understanding GPS: Principles and Applications," Second Edition*, Chapter 5, P. Ward, J. Betz, and C. Hegarty, "Satellite Signal Acquisition, Tracking, and Data Demodulation," Artech House, Publishers, 2005

[2] Kaplan, E., and C. Hegarty, editors, *Understanding GPS: Principles and Applications, Second Edition*, Chapter 6, P. Ward, J. Betz, and C. Hegarty, "Interference, Multipath, and Scintillation," Artech House Publishers, 2005

[3] Whitlow, Dana, "Design and Operation of Automatic Gain Control Loops for Receivers in Modern Communication Systems," Analog Devices 2007 Website Tutorial, Beaverton, Oregon

## Author

**Phil Ward** is president of Navward GPS Consulting, which he founded in 1991 in Dallas, Texas. Prior to becoming a consultant, he was senior member of the technical staff in the Defense Systems & Electronics Group of Texas Instruments Inc. Ward has been involved in the field of navigation since 1958 and with GPS receiver design as a systems engineer since 1976. He was the first Institute of Navigation (ION) Congressional Fellow (2001), the chair of the ION Satellite Division (1994-96), and ION President (1992-93). He received the ION Thurlow Award (1989) for developing the first commercial GPS receiver, the TI 4100. Ward received his B.S.E.E. degree from the University of Texas at El Paso and his M.S.E.E. degree from Southern Methodist University in Dallas, Texas. He also took postgraduate courses in Computer Science at Massachusetts Institute of Technology (MIT) while a member of the technical staff on the Apollo Guidance Computer design team at the MIT Instrumentation Lab, now Charles Stark Draper Lab (1967-70). **IG**